Fractional adiabatic passage in two-level systems: Mirrors and beam splitters for atomic interferometry

James Bateman* and Tim Freegarde
School of Physics and Astronomy, University of Southampton, Southampton, SO17 1BJ, United Kingdom
(Received 23 February 2007; published 24 July 2007)

Atom interferometers require atom mirrors and beam splitters that can maintain high fidelity even when experimental parameters vary from the ideal. We address the use of chirped laser pulses to provide such elements via rapid adiabatic passage, and present a prescription for practical pulses that offer controlled adiabaticity throughout. Full- and half-adiabatic pulses, providing mirrors and beam splitters, respectively, are derived, and the latter examined for robustness and suitability for experimental implementations.

DOI: 10.1103/PhysRevA.76.013416 PACS number(s): 32.80.Qk, 39.20.+q

I. INTRODUCTION

The central elements of an optical interferometer are the mirrors and beam splitters that deflect, divide, and recombine the incident light. In an atom interferometer [1,2], the corresponding elements are those that, respectively, switch prepared atoms between a pair of quantum states, and convert between either of the two eigenstates and equal superpositions of defined relative phase. The simplest implementations couple the two states using an optical field which, when resonant, results in Rabi oscillations. With judicious control of the optical intensity and duration, so that the interaction lasts just a half or quarter Rabi cycle, simple laser pulses achieve the required operations. The Rabi frequency depends, however, upon the laser intensity and apparent frequency, which vary with the position and Doppler shift of the atoms in the laser beam. While simple interferometers are possible, variations in the prepared state can be significant.

Rapid adiabatic passage (AP) [3–6]—which is quick in comparison with any incoherent processes (such as spontaneous emission) but slow in comparison with the Rabi oscillation—depends on off-resonant coupling of the two states and achieves a steady-state superposition that depends upon the detuning between the laser and the atomic resonance. By varying the detuning slowly, population can be transferred with arbitrary fidelity from one state to the other. In the common Feynman, Vernon, and Hellwarth pseudopolarization representation [7] of a two-level superposition as a "state vector," the superposition precesses about an adjustable "field vector" defined by the phase, intensity, and detuning of the optical field. Provided that the field vector is varied sufficiently slowly, the angle between it and the precessing state vector remains fixed. Control of the azimuthal angle of the state vector around the field vector is lost during such an operation, but if the vectors are initially aligned, the azimuthal angle is inconsequential. A less than perfectly adiabatic operation, however, introduces an uncontrolled change in the angle between the vectors and hence increases the parameter space to which the state is mapped; this renders the process irreversible and nonadiabatic.

Given initial alignment of the state and field vectors and a sufficiently slow variation of the latter, the superposition can be made to follow an essentially arbitrary path: the state vector remains at all times parallel to the field vector, and the evolution is deterministic and adiabatic. For the mirrors of an atom interferometer, this path usually leads from one eigenstate to the other—it causes the complete inversion of the atomic population and, since the initial and final field vectors correspond to large detuning and zero intensity, the process is extremely insensitive to experimental variations. For the beam splitters, however, the path instead ends or begins with an equal superposition: the final field must be exactly resonant, and the process is somewhat less robust.

In practice, the slow variation of the field vector desired for adiabaticity must be weighed against the need to complete the operation (and indeed the interferometry itself) before spontaneous emission and other processes of decoherence can occur. There may also be constraints from the finite duration of the atoms within the apparatus, or the accrual of, for example, velocity-dependent phases. Simple implementations of rapid adiabatic passage, such as linear chirps at constant intensity, satisfy the adiabaticity criterion to varying extents at different stages of the operation, and the overall fidelity can be far from optimum for the particular experimental constraints. Furthermore, the common method of creating superpositions—simply by truncating a pulse that would otherwise have caused complete population inversion (e.g., Ref. [8])—is far from adiabatic during the final extinction and can be highly sensitive to experimental variations. In this paper, we therefore consider the design and optimization of mirror and beam-splitter pulses that maintain uniform adiabaticity, and hence reduce the sensitivity of such processes to variations in experimental parameters.

Our attempt to control adiabaticity throughout a pulse is not the first [9,10]—a well known pulse for which the adiabaticity is constant is the tangent frequency sweep [11], for which one uses a constant intensity (or some other appropriate measure of coupling strength) while the frequency difference from resonance follows an inverse-tangent sweep in time. We shall see that, as is demonstrated by this example, the necessary condition that the detuning from resonance relative to the coupling strength be large at the beginning and end of the operation means any "pulse" employing constant intensity throughout inescapably requires a large, perhaps impractically so, frequency range. Furthermore, we are unaware of any attempt to derive a pulse of constant adiabatic-

*jbateman@soton.ac.uk

ity for the more challenging case of fractional, rather than full, adiabatic passage.

In this paper, we extend the idea of constant adiabaticity for constant intensity to any form of controlled adiabaticity for, crucially, a smoothly modulated intensity. As well as reducing considerably the required frequency range, the inclusion of the extinction in the pulse design now allows us to consider pulses for half, as well as full, adiabatic passage.

II. CONTROLLED ADIABATICITY PULSE

Our analysis addresses the coupling of two nondegenerate quantum states, labeled $|0\rangle$ and $|1\rangle$, by a near-resonant optical field that is described at any time by its amplitude and frequency, which we write in the form of a coupling strength (or Rabi frequency) $\Omega(t)$ and detuning from resonance $\Delta(t)$. For the example of an electric dipole transition in an atom, the coupling strength, in terms of the time-dependent amplitude of the electric field $E(t)$, the atomic transition frequency ω_0, and the dipole matrix element $e\langle 1|\hat{x}|0\rangle$, is [12]

$$\Omega(t) = \frac{e\langle 1|\hat{x}|0\rangle}{\hbar} E(t),$$

$$\Delta(t) = \omega(t) - \omega_0,$$

where $\omega(t)$ is the time-dependent excitation frequency.

In the Feynman pseudopolarization representation [7] the quadrature sum of these parameters $\tilde{\Omega} = \sqrt{\Omega^2 + \Delta^2}$ is the rate of precession of the state vector around the field vector, and the angle θ between the field vector and the vertical (eigenstate) is given by $\tan\theta = \Omega/\Delta$ [30]. These parameters are the same as occur in the dressed states treatment, corresponding, respectively, to the energy splitting of the dressed states and the mapping of bare states on to dressed states [12,13].

The condition for adiabaticity is that the rate of precession $\tilde{\Omega}$ be much greater than the rate of rotation of the field vector $\dot{\theta} \equiv d\theta/dt$ [12,14]. A common measure is the adiabatic parameter $Q(t)$ [15] which, together for later convenience with its reciprocal $\epsilon(t)$, is defined by

$$Q(t) \equiv 1/\epsilon(t) \equiv \tilde{\Omega}/\dot{\theta}. \tag{1}$$

When $Q \to \infty$ ($\epsilon \to 0$) the process is adiabatic. It follows that the time-dependent field parameters Ω and Δ are linked by this adiabatic parameter.

Our strategy is to take an experimentally straightforward amplitude Ω, constrain the adiabatic parameter ϵ to a given function, and hence derive the required frequency chirp Δ. The converse (where Δ is set and Ω calculated) is similarly possible, and follows the same procedure.

A. General properties of the pulse

We begin by noting that the relationships between θ and Ω and Δ may also be written as

$$\sin\theta = \left(\frac{\Omega}{\tilde{\Omega}}\right), \quad \cos\theta = \left(\frac{\Delta}{\tilde{\Omega}}\right), \quad \tan\theta = \left(\frac{\Omega}{\Delta}\right), \tag{2}$$

from which, using the definition of ϵ, we construct a differential equation as follows:

$$\dot{\theta} = \epsilon\tilde{\Omega},$$

$$\Rightarrow \dot{\theta}\sin\theta = \epsilon\tilde{\Omega}\left(\frac{\Omega}{\tilde{\Omega}}\right) = \epsilon\Omega, \tag{3}$$

with no specific constraint yet applied to the adiabatic parameter ϵ. We integrate from the time t_h at which detuning is zero and the field vector is horizontal [$\Delta(t_h)=0$] to find an expression for $\cos\theta$, which, for brevity, we label as $\Gamma(t)$.

$$[\cos\theta(t')]_{t_h}^{t} = -\int_{t_h}^{t} \dot{\theta}(t')\sin\theta(t')dt'$$

$$= \int_{t}^{t_h} \epsilon(t')\Omega(t')dt' \equiv \Gamma(t). \tag{4}$$

Then, using Eq. (2), we find Δ in terms of Ω as follows:

$$\Delta(t) = \frac{\Omega}{[\tan\theta(t')]_{t_h}^{t}} = \frac{\pm\Omega\Gamma}{\sqrt{1-\Gamma^2}}. \tag{5}$$

In addition to t_h, for which $\theta(t_h)=\pi/2$, we introduce t_v for which $\theta(t_v)=0$, the latter corresponding to a field vector aligned with the vertical (eigenstate). With this definition, the integral in Eq. (4) becomes

$$\int_{t_v}^{t_h} \epsilon(t)\Omega(t)dt = 1. \tag{6}$$

This integral is a general result for adiabatic following. It implies the constraint that, given $\Omega(t)$, a decrease in $\epsilon(t)$ [due, for example, to a change in some parameter affecting the detuning function $\Delta(t)$] necessitates an increase in $\epsilon(t)$ elsewhere. Examples of this behavior occur later when we consider modifications to derived pulse forms, and their imperfect experimental implementations.

B. Cosine-squared envelope

As an example of smooth modulation, we consider an experimentally realizable, cosine-squared pulse envelope and constant adiabaticity as follows:

$$\Omega(t) = \Omega_0 \cos^2\left(\frac{\pi t}{2\tau}\right), \quad -\tau \leqslant t \leqslant +\tau,$$

$$\epsilon(t) = \epsilon_0.$$

Additionally, if we choose the initial field vector to be vertical (that is, aligned with the eigenstate), $t_v=-\tau$ and the expression in Eq. (6) becomes

$$\frac{\epsilon_0\Omega_0}{2}\left[t + \frac{\tau\sin\left(\frac{\pi t}{\tau}\right)}{\pi}\right]_{t_v=-\tau}^{t_h} = 1. \tag{7}$$

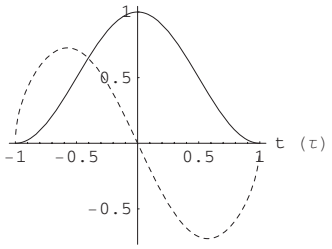

FIG. 1. Coupling strength Ω (Ω_0) (solid) and detuning Δ (Ω_0) (dashed) for full AP "mirror" pulse of duration 2τ. The frequency detuning is adapted throughout to maintain constant adiabaticity as the coupling strength follows an experimentally convenient $\cos^2$ profile.

These general relationships can now be used to construct specific pulses, such as those necessary to invert a state or to create a superposition simply by choosing the time t_h at which resonance should occur.

1. Full adiabatic passage (mirror)

For our "full AP" pulse, we begin, in the Feynman representation, with the field vector aligned with one pole (eigenstate) and sweep it to the other. Resonance occurs midway, at $t=0$, and hence the relevant condition is $t_h=0$. With this condition, Eq. (7) becomes $\epsilon_0\Omega_0\tau=2$, and

$$\Gamma(t)=\frac{t}{\tau}+\frac{1}{\pi}\sin\left(\frac{\pi t}{\tau}\right), \tag{8}$$

from which $\Delta(t)$ follows using Eq. (5), and is illustrated in Fig. 1. A sharp initial rise in detuning peaks at $t_{\max}\approx\mp 0.575\tau$ at a detuning of $\Delta(t_{\max})\approx\pm 0.727\Omega_0$. The frequency modulation is symmetrical, and the maximum phase excursion—the maximum of the integral of detuning—is $\Phi_{\max}=1/\epsilon_0$; overall, the excursion is zero.

The shape of this detuning function is similar to that from a self-phase modulated pulse and the possibility of using an SPM pulse to perform the mirror operation is discussed further in Sec. II C 1.

2. Half adiabatic passage (beam splitters)

Using an identical procedure, we can derive a pulse which performs a "half AP" operation. For this, the detuning must end on zero, and hence the condition is $t_h=\tau$. The relationship in Eq. (7) is then simply $\epsilon_0\Omega_0\tau=1$ and, using this,

$$\Gamma(t)=\frac{1}{2}\left[1-\frac{t}{\tau}-\frac{1}{\pi}\sin\left(\frac{\pi t}{\tau}\right)\right]. \tag{9}$$

The corresponding detuning function, again obtained from Eq. (5), is illustrated in Fig. 2. Again, there is a sharp initial rise in detuning, which peaks at $t_{\max}\approx-0.506\tau$ at $\Delta(t_{\max})\approx 1.09\Omega_0$. The total phase excursion is $\Phi_{\max}\approx 0.866/\epsilon_0$.

In contrast to the Rabi $\pi/2$ pulse, which we consider further in Sec. II D, the beam-splitter and recombiner pulses based on AP are not identical. The recombiner can be regarded as the continuation of the beam splitter that would complete the adiabatic inversion, or simply its time reversal; in both cases, the recombiner pulse sweeps from on resonance to far off resonance.

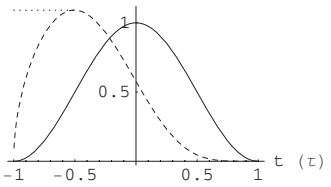

FIG. 2. Coupling strength Ω (Ω_0) (solid) and detuning Δ (Ω_0) (dashed) for half AP "beam-splitter" pulse of duration 2τ. As before, the frequency detuning is adapted throughout to maintain constant adiabaticity and the form of $\Delta(t)$ during the extinction ensures the superposition is approached adiabatically. The constant detuning (dotted) preceding the peak of the ideal function is a pragmatic modification, and is discussed in the text.

C. Comparison with traditional chirp schemes

Having determined the constant-adiabaticity frequency modulation for the mirror and beam-splitter operations, we find it instructive to compare them with established techniques.

1. Full adiabatic passage

The simplest method for performing adiabatic inversion might consist of a constant coupling amplitude $\Omega(t)=\Omega_0$ and a frequency sweep from well above to well below resonance. Unfortunately, for the initial and final field vectors to be aligned with the eigenstates, $\Delta(t)$ must sweep over a range much larger than the coupling strength: $\Delta_{\max}\gg\Omega_0$. Inescapably, this approach requires an unreasonably large maximum detuning, even before any considerations of adiabaticity.

The situation is improved significantly by moving to a smooth modulation, such as the cosine-squared envelope previously described. For the simplest form of frequency chirp (a linear temporal chirp) the adiabatic parameter does vary during the pulse, but for the case of $\Delta_0\approx 2\Omega_0$ (which gives the same chirp rate at the middle of the pulse as our constant adiabaticity case), $\epsilon(t)$ does not significantly exceed that of the derived constant adiabaticity pulse. For small (large) chirp rates, there are significant peaks in adiabaticity at the ends (middle) of the pulse, as shown in Fig. 3. [Such increases in $\epsilon(t)$ are unavoidable, as embodied by Eq. (6).]

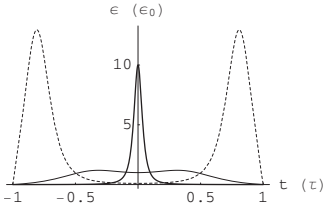

FIG. 3. Variation of the adiabatic parameter $\epsilon(t)$, relative to the ideal $\epsilon_0=2(\Omega_0\tau)^{-1}$, during a linear temporally chirped pulse $\Delta(t)=\Delta_0 t/\tau$ with a smooth cosine-squared intensity modulation $\Omega(t)=\Omega_0\cos^2[(\pi t)/(2\tau)]$. The three cases correspond to $\Delta_0=2\Omega_0$ (solid), $\Delta_0=20\Omega_0$ (thick), and $\Delta_0=0.2\Omega_0$ (dashed).

For these cases, the state will not adiabatically follow the field and the pulse will not be experimentally useful. However, adiabatic inversion has been studied extensively, and there are many smoothly modulated pulse types which are robust [16].

We thus conclude that, while the precise pulse shape and chirp form are of limited consequence, a smoothly modulated pulse is important for full AP operations and makes far more efficient use of the available experimental resources. The form of Fig. 1 suggests that appropriate pulses might be provided by, for example, self-phase modulation of an ultrashort laser pulse; several such implementations have been considered in detail by Goswami and Warren [17].

2. Half adiabatic passage

The remarkable robustness of adiabatic inversion is not, unfortunately, shared by half adiabatic passage, for which the form of approach to resonance, and simultaneous extinction, is crucial. The simple truncation of a pulse will be far from adiabatic, and will also be sensitive to frequency errors that cause a non-zero final detuning. Conversely, pulses with no distinct end, such as a Gaussian intensity envelope, may approach resonance adiabatically but remain there long enough for small perturbations to accrue. The optimum pulse must have a definite end, but should approach resonance in a controlled manner.

D. Practical beam-splitter pulses

We now focus on the practicalities of the half AP pulse, derived in Sec. II B 2 and shown in Fig. 2. No real pulse will match the required pulse form; the dominant imperfections are likely to be variations in the Rabi frequency, due to intensity variations across a laser beam profile, and frequency shifts due, for example, to the various Doppler shifts for atoms within a thermal cloud. We consider these effects by introducing a coupling strength scaling factor α, and a frequency offset f, in the natural units of the problem, Ω_0. For our practical pulse, we therefore model the coupling strength and detuning functions by

$$\Omega_e(t) = \alpha\Omega(t), \tag{10}$$

$$\Delta_e(t) = \Delta(t) + f\Omega_0. \tag{11}$$

The ideal pulse is given by $\alpha=1$ and $f=0$. A nonideal pulse will result in a nonequal superposition and/or an error in the relative phase of the two components. We shall measure the fidelity of the superposition and phase errors using the definitions

$$q \equiv 1 - 2\left|\frac{1}{2} - |\langle 0|\psi\rangle|^2\right|, \tag{12}$$

$$\sin(\chi) \equiv \mathrm{Im}\,\frac{\langle 1|\psi\rangle}{\langle 0|\psi\rangle}\left|\frac{\langle 0|\psi\rangle}{\langle 1|\psi\rangle}\right|, \tag{13}$$

where $|\psi\rangle$ is the state of the system after the pulse. Before proceeding, we make one pragmatic modification. Because the derived pulse of Fig. 2 begins with zero detuning, the initial direction of the field vector is extremely sensitive to errors in Δ and Ω. As the condition for field vector alignment with the eigenstate is $\Delta(-\tau) \gg \Omega(-\tau)$, we amend the form of $\Delta_e(t)$ so that the detuning begins at, and initially maintains, its peak value as follows:

$$\Delta_m(t) = \begin{cases} \Delta_e(t_{\max}) = 1.092\Omega_0 + f\Omega_0 & t < t_{\max}, \\ \Delta_e(t) & t \geqslant t_{\max}. \end{cases} \tag{14}$$

This modification guarantees the initial field vector alignment (provided f is greater than ≈ -1) at the expense of a small ($<10\%$) variation in the adiabatic parameter $\epsilon(t)$, which is unlikely to be of experimental significance. More important is the behavior as Δ and Ω approach zero at the end of the pulse, which is unaffected by this modification. Other modifications are possible, and this example is intended to illustrate the ability to meet both the constraints on ϵ and practical experimental requirements.

1. Realistic Rabi $\pi/2$ pulses

As a benchmark, we first consider the effect of experimental variations on the effect of a controlled area Rabi pulse characterized by a constant, resonant frequency and steady intensity which, in the notation of this paper, is described by

$$\Omega_e(t) = \alpha\Omega_0,$$

$$\Delta_e(t) = f\Omega_0,$$

$$\Omega_0\tau = \pi/2.$$

The error in superposition composition is calculated analytically, and is shown, as a function of the coupling and detuning variations α and f, in Fig. 4(a). The plot shows numerous regions where an equal superposition is created (white). Along the axis $f=0$ we see Rabi oscillations, with an equal superposition every odd integer multiple of a $\pi/2$ pulse. The behavior away from the $f=0$ axis may be understood by noting that, in the Feynman representation, the state vector is rotated about a vector that is inclined to the equator. The phase error of the superposition, shown for convenience by its sine in Fig. 4(b), manifests an essentially similar structure. In both cases, the key characteristic is relative tolerance of variations in frequency, but sensitivity to variations in coupling strength.

2. Realistic half AP pulse

We now consider the effect of experimental imperfections on our modified constant-adiabaticity pulses, whose ideal form is illustrated in Fig. 2, modified according to Eq. (14), and has imperfections described by Eqs. (10) and (11). Our results, shown in Fig. 5, are determined by numerical integration of the Schrödinger equation (specifically, the dressed states evolution), using the second order trapezoidal method [18], for a range of α and f. A value of $\epsilon_0 \sim 10^{-3}$ was chosen, but most of the features are not critically dependent on this parameter.

For imperfect pulses $(\alpha, f) \neq (1, 0)$, we cannot assume the adiabatic condition to be met throughout; the adiabatic pa-

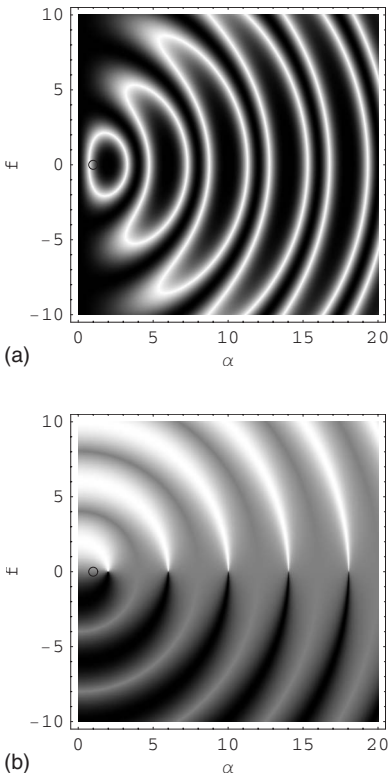

FIG. 4. (a) Fidelity q and (b) phase relative to the ideal $\sin(\chi)$ of the imperfect Rabi $\pi/2$ pulse, calculated analytically, with imperfections parametrized by a scaling of the coupling strength α and an offset of the resonance frequency $f\Omega_0$. Around the ideal pulse, circled at $\alpha=1$ and $f=0$, the fidelity follows the familiar Rabi oscillations for increasing coupling strength, and is relatively insensitive to frequency offsets; phase shows a similar structure. White is high and black is low.

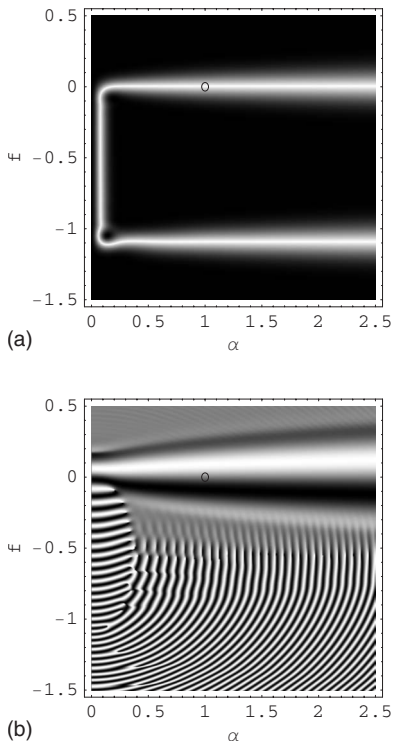

FIG. 5. The equivalent plot for an imperfect "half AP" pulse, based on the constant adiabaticity pulse, with a modification to avoid initial sensitivity to an offset in detuning, calculated by numerical integration with $\epsilon_0 \sim 10^{-3}$. In contrast to the Rabi controlled area pulse, a large fraction of the parameter space for this pulse leaves the state unaffected; only the smaller, interesting region is shown. (a) Fidelity q shows, as expected, a narrow branch around $f=0$ for which, above a minimum α, an equal superposition is created with (b) relative phase $\sin\chi$ unaffected by changing α but strongly dependent on f. The unexpected lower branch, centered on $f=-1.09$, for which fidelity is high and phase is rapidly varying, is discussed in the text. White is high and black is low.

rameter will not remain constant and, for $f \neq 0$, the pulse will be strongly nonadiabatic towards the end where $\Omega_e \to 0$ and the offset in detuning becomes significant. The field vector in this case adiabatically approaches the equator while the rate of precession reduces, but the vector then swings violently (nonadiabatically) back to point towards the pole before the pulse is fully extinguished. We shall see later, in Sec. II D 4, that this is similar to the second crossing in Stark-chirped rapid adiabatic passage (SCRAP). Although this increase in ϵ will in many cases be rapid and too short lived for the atom to respond significantly, it is clear that the practical optimum will combine the best adiabaticity during the pulse with the greatest tolerance to experimental uncertainties at the beginning and end.

The error in superposition for the half AP pulse is shown in Fig. 5(a). As expected, there is a narrow region, close to the $f=0$ axis, around which an equal superposition is created. Above a minimum coupling strength, the evolution is adiabatic and a further increase in coupling strength merely increases this adiabaticity.

If we assume that most imperfections accrue during the final extinction of the pulse we are able to offer an approximate description for this branch. We take the perturbation to begin at a time t_f when the detuning $\Delta_m(t_f) \sim \Omega_e(t_f)$—that is, the field vector lies at 45° to its ideal direction—and the detuning function is dominated by the frequency error, $\Delta_m(t_f) \approx f\Omega_0 \sim \alpha\Omega_0 \cos^2[(\pi t_f)/(2\tau)]$. We estimate the subsequent precession of the state vector by approximating the field vector to a constant for the remainder of the pulse, and, by imposing that this precession ϕ must be small, deduce the following:

$$\phi = \int_{t_f}^{\tau} \tilde{\Omega}(t)dt \sim \Omega(t_f)(\tau - t_f) \sim f\Omega_0\tau\frac{2}{\pi}\left(\frac{\pi}{2} - \arccos\sqrt{\frac{f}{\alpha}}\right)$$

$$\sim \Omega_0\tau\sqrt{\frac{f^3}{\alpha}} \ll 1.$$

The region of high fidelity in Fig. 5(a) is hence described by

$$\sqrt{\frac{f^3}{\alpha}} \ll \epsilon_0. \tag{15}$$

There is a further region, also achieving an equal superposition, centered around a negative detuning offset of $f=-1.09$, corresponding to the case in which the initial detuning $\Delta_m(-\tau)$ is zero. For this pulse, the field vector begins on the

equator, at right angles to the state vector, before moving adiabatically towards the pole. The angle between state and field vectors remains constant during this evolution, but the azimuthal angle of the state vector relative to the field vector precesses rapidly. When the field vector comes to rest, the state is in an equal superposition, but the phase is undetermined. Superficially, this appears similar to the "recombiner" pulse, but the detuning in this branch is not such that constant adiabaticity is maintained, and no consideration has been given to the phase of the initial (azimuthal) angle of the field vector along the equator. Figure 5(a) also shows a vertical (constant α) band joining the upper and lower branches: this is dependent on the adiabatic parameter ϵ_0, and is not experimentally useful.

The phase error for the half AP pulse is shown in Fig. 5(b). This shows quite different behavior for the on- and off-resonance branches, with a region of slowly varying phase surrounding the on-resonance branch while, in stark contrast, the off-resonance branch falls in a region of rapidly varying phase. The upper branch is therefore useful; the lower branch is not.

3. Comparison of sensitivity to imperfections

The Rabi half AP pulses differ markedly in their tolerance to experimental variations, with the Rabi pulse being relatively tolerant of variations in frequency but sensitive to coupling strength, while the AP pulse offers tolerance to coupling strength at the expense of an increased frequency dependence. Specifically, while the Rabi pulse dependence on intensity variations about the ideal shows the familiar oscillation, the AP pulse is essentially unaffected by changes in coupling strength once the adiabatic regime is reached (for the example illustrated in Fig. 5, this is when $\alpha > 0.2$). This insensitivity to coupling strength is the familiar advantage of the adiabatic approach. The change in phase with coupling strength, provided there is no frequency error, is in both cases zero. The dependence of superposition phase on the frequency error, however, is much stronger for the AP pulse than for the Rabi pulse.

To illustrate the relative sensitivities of the two approaches to experimental variations, we consider a typical example of coherent atomic manipulation. Extending the example in Sec. II of an atomic dipole, we consider the transition $5S_{1/2} \rightarrow 5P_{3/2}$ in a laser-cooled sample of ^{85}Rb, at a temperature of (typically) <100 μK [19], for which the Doppler width is approximately 150 kHz. If the coupling is provided by a 100 mW laser, focused to a spot $w_0 = 1$ mm, the (maximum) Rabi frequency is $\Omega_1 \approx 2\pi \times 350$ MHz. The two hyperfine states of the $5S_{1/2}$ state can be coupled using two such beams (slightly detuned from the single-photon resonance, and with a frequency difference equal to the hyperfine splitting) to drive a resonantly enhanced Raman transition [20,21]. The coupling strength for this two-photon process is [22]

$$\Omega_2 = \frac{\Omega_1 \times \Omega_1}{2\delta} \approx 2\pi \times 60 \text{ MHz}$$

for $\delta \gg \Omega_1$, where we have taken a typical single-photon detuning of $\delta = 2\pi \times 1$ GHz and the subscript refers to the number of photons involved in the process.

For this example, the insensitivity to coupling strength vastly increases the usable area of the beam. If we can accept an error of 1% in the superposition $q > 0.99$, the Rabi approach works over only a small region near the center of the Gaussian beam profile, extending to approximately 10% of the beam waist, and encompassing 2% of the power. This also assumes there is no jitter in the pulse duration. In contrast, the adiabatic approach, for which we can allow α to be as low as 0.2 (for the typical parameter $\epsilon \sim 10^{-3}$ used in these calculations, with a smaller adiabatic parameter permitting a further excursion towards $\alpha = 0$), extends the useful region to nearly 90% of the beam waist, encompassing 80% of the power.

The dependence of superposition phase on the frequency offset f, for $\alpha = 1$, is small for Rabi pulses, $\partial\chi/\partial f = 1$, while the AP pulse rests on a steep slope with $\partial\chi/\partial f \approx 18$. In our example, the range of f will be determined by Doppler shifts for the thermal sample, with a typical value of

$$f \approx \pm \frac{2\pi \times 300 \text{ kHz}}{\Omega_2} \approx \pm 5 \times 10^{-3}. \tag{16}$$

(The worst case of counterpropagating Raman beams is chosen, for which the total Doppler shift is the sum of that for each beam. The copropagating arrangement is, to first order, Doppler insensitive.) Hence, at $\alpha = 1$, the phase uncertainty is $\delta\chi \approx 5°$, compared with the Rabi case of $\delta\chi \approx 0.3°$. While the cumulative error arising from this uncertainty may be unacceptable for complex interferometers, the increased frequency sensitivity will, for many applications, be less significant than the benefits accompanying the insensitivity to coupling strength.

Although the frequency and intensity errors will often be systematic, we have also examined the case of small random variations and their effect on a simple two-pulse interferometer: the dependence on α may generally be neglected, but variations in frequency lead to a reduction in the fringe visibility. If f is normally distributed about zero with a width σ_f, the visibility shows an approximately Gaussian dependence on σ_f, falling to $\frac{1}{2}$ at $\sigma_f \sim 0.01$, for the typical adiabatic parameter $\epsilon_0 \sim 10^{-3}$.

The analysis above shows the Rabi approach to be favorable if detuning is uncertain, and the AP approach to be best if coupling strength is uncertain. The key observation is that in many experimental situations (such as cold atom and ion experiments), the frequency can be controlled far better than the coupling strength.

4. Relation to other adiabatic techniques

The description adopted in this paper, in terms of the parameters of detuning and coupling strength, can be applied to many implementations of adiabatic passage, which involve time-delayed pulse pairs to achieve similar effects. A particularly close analogue is found in Stark-chirped rapid adiabatic passage (SCRAP) [23,24], where two pulses impinge on a two-level system such that one (on-resonance) couples the states while the other (far off-resonance) provides a time-dependent detuning via the ac Stark shift. For full population transfer, the Stark (or detuning) pulse is delayed slightly rela-

tive to the coupling pulse, resulting in adiabatic following from the initial to the final eigenstate, and then a nonadiabatic return of the field to the starting position, *without being followed* by the state. SCRAP has also been adapted to create superpositions [25].

Additionally, there appears to be an interesting similarity between the pulse derived here and recent work by Vitanov *et al.* [26], where stimulated rapid adiabatic passage (STIRAP) is recast in terms of a two-level system; see also [27]. The authors show a detuning and a coupling pulse displaced in time (Fig. 2 in [26]) which, while an accurate model of their system, shows a strongly nonuniform adiabatic parameter at early and late times. This recasting of STIRAP also suggests that it may be possible to describe fractional STIRAP [28,29] in similar terms to the example pulse in this paper.

Finally, we observe that simply constraining the adiabatic parameter is perhaps naïve. The adiabatic parameter varies significantly in the time displaced Gaussians of Vitanov's work, but it does so only when the coupling strength is weak, and hence does not adversely affect the operation. A more complete approach to finding an optimum adiabatic pulse might proceed by establishing some measure of deviation from ideal adiabatic behavior, and then finding the function which minimizes it, while also ensuring tolerance of experimental uncertainties, and accounting for experimentally limited parameters such as the maximum practical detuning and the finite time allowed for the pulse.

III. CONCLUSIONS

We have addressed the use of adiabatic passage for mirrors and beam splitters in atom interferometry and the possibility of tailoring the combination of frequency and amplitude modulation to control the adiabaticity during the pulse. We have presented a straightforward analytical approach, which leads to expressions of direct use for the frequency modulation of an experimentally realizable pulse and which can readily be applied to experimental implementations. In comparison with the linear temporal chirp and inverse tangent sweep, our smooth modulation and tailored chirp achieves better fidelity within experimental constraints. By observing the adiabaticity throughout the pulse, our approach also offers insight into related processes such as SCRAP and STIRAP.

We have examined the sensitivity of these pulses to experimental variations in frequency and intensity of the excitation. In particular, for the experimentally challenging case of the beam splitter, we have compared our tailored approach with the simple half Rabi cycle. Although the half Rabi pulse has a greater tolerance of variations in frequency, the chirp proves far more robust against variations in intensity, which are likely to be more problematic experimentally and result from variation across a beam profile as well laser intensity fluctuations. The effect of an imperfect adiabatic beam splitter is understood simply using the Feynman representation and considering the deviation of the field vector during the final extinction of the pulse.

The inclusion of the extinction in the design procedure proves crucial: to our knowledge, this is the first application of controlled adiabaticity to the design of a half-adiabatic-passage pulse, and the first example of a pulse which can robustly create superpositions in a two-level system with a single exciting field.

ACKNOWLEDGMENTS

We gratefully acknowledge the support of EPSRC Grant No. GR/S71132/01.

APPENDIX: ADIABATIC PASSAGE AND ROTATIONS

Our technique is designed to mimic, in the language of quantum computing, a qubit rotation, and so it is important to assess the differences between adiabatic evolution and a rotation of the state vector in the Feynman representation [7]. We approach this by considering the rotation of the basis necessary to move from bare states to dressed states, followed by the adiabatic evolution of these dressed states, and finally the rotation from dressed states back to bare states [12]. The result is that, for adiabatic following, only the phase of the overlap of the state with the (time-dependent) dressed eigenstates changes in time. This corresponds to the familiar result that the angle between state and field vectors remains constant (e.g., Ref. [22]), but is derived here independently of this geometrical representation. This result is used to assess the suitability of adiabatic beam-splitter and mirror pulses for interferometry.

1. Adiabatic evolution of dressed states

Consider a two-level system with coupling strength described by the Rabi frequency Ω, which varies (slowly) in time. This coupling is detuned from resonance by (Δ), which is also permitted to vary in time. The bare states of a system $|0\rangle$ and $|1\rangle$ can be rotated to form the dressed states $|-\rangle$ and $|+\rangle$ by

$$\begin{pmatrix} |-\rangle \\ |+\rangle \end{pmatrix} = \begin{pmatrix} \cos(\theta/2) & -\sin(\theta/2)e^{i\rho} \\ \sin(\theta/2)e^{-i\rho} & \cos(\theta/2) \end{pmatrix} \begin{pmatrix} |0\rangle \\ |1\rangle \end{pmatrix}, \quad \text{(A1)}$$

where $\tan\theta = \Omega/\Delta$ and ρ is the relative phase of system and perturbation. We use the FM frame [10], for which ρ is constant throughout the pulse, and we choose $\rho = 0$. The coefficients ($A_{0,1}$ and $A_{-,+}$) transform in the same way, and their evolution is described by

$$\frac{d}{dt}\begin{pmatrix} A_- \\ A_+ \end{pmatrix} = \frac{i}{2}\begin{pmatrix} \tilde{\Omega} & i\dot{\theta} \\ -i\dot{\theta} & -\tilde{\Omega} \end{pmatrix}\begin{pmatrix} A_- \\ A_+ \end{pmatrix}, \quad \text{(A2)}$$

where (as before) $\tilde{\Omega} = \sqrt{\Omega^2 + \Delta^2}$ and an overdot indicates the time derivative. In the adiabatic approximation ($\dot{\theta} \to 0$) [12] this integrates to

$$\begin{pmatrix} A_-(t) \\ A_+(t) \end{pmatrix} = \begin{pmatrix} e^{+i\phi/2} & 0 \\ 0 & e^{-i\phi/2} \end{pmatrix}\begin{pmatrix} A_-(0) \\ A_+(0) \end{pmatrix}, \quad \text{(A3)}$$

$$\text{where } \phi = \int_0^t \tilde{\Omega}(t')dt'. \quad \text{(A4)}$$

We use R_t to represent the rotation matrix of Eq. (A1), with the subscript t reflecting the time dependence inherited from

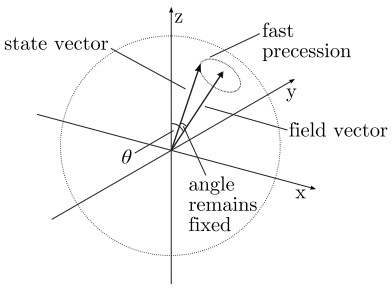

FIG. 6. Adiabatic following in the Feynman representation.

θ. B and D represent the (time-dependent) column vectors of bare and dressed states, respectively, with the equivalent kets $|B\rangle$ and $|D\rangle$, where appropriate. Finally, $T_{b,a}$ represents the adiabatic evolution of the dressed states in Eq. (A3) between times a and b. In this representation,

$$D_t = R_t B_t,$$

$$D_t = T_{t,0} D_0. \tag{A5}$$

The final bare-state amplitudes are hence obtained by

$$B_t = R_t^{-1} T_{t,0} R_0 B_0. \tag{A6}$$

2. Time-evolution of overlap with a test state

To illustrate, we use a test state $|S\rangle$, and find the overlap $\sigma_t = \langle S|B_t\rangle = S^\dagger B_t$. If $S=(1,0)^T$, $B_0=(1,0)^T$, and $\theta_t=\theta_0=\theta$ then, using Eq. (A6),

$$\sigma_t = \cos(\phi/2) + i \sin(\phi/2)\cos(\theta). \tag{A7}$$

For on-resonance excitation, $\cos(\theta)=0$ and, using $\tilde{\Omega}=\Omega$ in Eq. (A4), we recover Rabi flopping: $|\langle S|B_t\rangle|^2=\cos^2(\Omega t/2)$. The oscillation depth reduces for $\cos(\theta)\neq 0$ and the procedure is similar for the overlap of B_t with any state in the bare-states representation.

A more useful result is found for the special case of projection along a dressed eigenstate. If U represents the dressed eigenstate in the dressed-state basis [i.e., $U=(1,0)^T$ or $(0,1)^T$] the projection is simply

$$\sigma_t = U^\dagger D_t = U^\dagger T_{t,0} R_0 B_0.$$

The equivalent S vector is $S_t=R_t^{-1}U$. In this basis, the product $U^\dagger T_{t,0}$ is trivial: $(e^{i\phi/2},0)$ or $(0,e^{-i\phi/2})$. That is, the only effect of time evolution on the projection σ_t is a phase evolution and $|\sigma_t|^2$ is independent of time.

So, adiabatic manipulation keeps the overlap of the state with the dressed eigenstates constant, and manipulation of the bare-state amplitudes can be achieved by altering the dressed eigenstates. When the initial state of an atom does not fully overlap with an initial dressed eigenstate, adiabatic manipulation introduces, via an uncontrolled phase, uncertainty in the (measurable) overlap with bare eigenstates. This behavior corresponds to the state vector remaining at a constant angle from the field vector, around which it rapidly rotates (see Fig. 6). To clarify this behavior, the next section compares an adiabatic beam splitter with a traditional $\pi/2$ pulse.

3. Comparison of AP and Rabi pulses

Consider first the classic Rabi $\pi/2$ pulse which, as neither frequency or intensity is changing, can be treated as adiabatic (except for the initial switch on and final extinction). Excitation is on resonance ($\theta=\pi/2$) and a well defined rotation is induced ($\phi=\pi/2$). The effect of two such pulses, with a time delay between them, acting on a system initially in a bare eigenstate is shown in Table I. The accrued phase γ is mapped to the probability of inversion; this is, of course, a simple interferometer.

Next, consider the effect of two half AP pulses used in the same way. The first half AP pulse sweeps from far off resonance to on resonance ($\theta=0\rightarrow\pi/2$), and induces a large and uncertain number of precessions around the field vector; this is recorded in the phase ϕ_1. The second pulse now sweeps from on resonance to far off resonance ($\theta=\pi/2\rightarrow\pi$), with a different large number of revolutions ϕ_2. This progress is also shown in Table I.

For AP pulses, the precession around the field vector ($\phi_{-,+}$) is unknown and so, while the probability of inversion is identical to that obtained using the Rabi pulses, any subsequent operation will be sensitive to this uncertain phase. Hence, we conclude that this manipulation technique may be limited to "interferometers" containing two "beam splitters"

TABLE I. Comparison of Rabi and AP based "$\pi/2$" pulses used to implement a simple interferometer. The state shown is that of the system after the stated operation. The state is initialized, the "beam-splitter" pulse is applied, the system is permitted to evolve freely and accrue some phase, and finally the "recombiner" pulse is applied to map this accrued phase to a (measurable) probability for each eigenstate.

Operation	$\pi/2$ Rabi pulses	AP based pulses
Initialize	$\|0\rangle$	$\|0\rangle$
First pulse	$\|0\rangle - i\|1\rangle$	$e^{i\phi_1/2}(\|0\rangle - \|1\rangle)$
Free evolution	$e^{i\gamma/2}\|0\rangle - ie^{-i\gamma/2}\|1\rangle$	$e^{i\phi_1/2}(e^{+i\gamma/2}\|0\rangle - e^{-i\gamma/2}\|1\rangle)$
Second pulse	$i \sin \gamma/2\|0\rangle - i \cos \gamma/2\|1\rangle$	$e^{i\phi_-/2} i \sin \gamma/2\|0\rangle - e^{i\phi_+/2} i \cos \gamma/2\|1\rangle$ where $\phi_- = \phi_1 - \phi_2$ and $\phi_+ = \phi_1 + \phi_2$

only: a splitter, and a recombiner—the inverse of a beam splitter in which the field vector sweeps adiabatically from horizontal to vertical.

In addition to beam splitters, mirrors are usually required to build an interferometer. As before, these may be implemented with controlled area Rabi pulses (π pulses), or full AP pulses. The Rabi version is a true rotation, but is experimentally fragile; the AP version, while robust, does not (in general) preserve the phase information recorded in γ. For example, the state following a half AP pulse and a full AP pulse is

$$e^{i\phi_1/2}(e^{-(\gamma+\phi_M)/2}|0\rangle - e^{+(\gamma+\phi_M)/2}|1\rangle),$$

where ϕ_M is the unknown phase of the full AP pulse.

All of these operations, including those of consecutive pulses, can be understood purely geometrically in the Feynman representation—one need only remember that, for any adiabatic operation, the angle between the state and the field vectors remains constant while the large and uncertain number of precessions loses all information about the azimuthal angle of the former around the latter.

[1] M. Weitz, B. C. Young, and S. Chu, Phys. Rev. Lett. **73**, 2563 (1994).

[2] J. Baudon, R. Mathevet, and J. Robert, J. Phys. B **32**, R173 (1999).

[3] B. W. Shore, K. Bergmann, A. Kuhn, S. Schiemann, J. Oreg, and J. H. Eberly, Phys. Rev. A **45**, 5297 (1992).

[4] J. S. Melinger, S. R. Gandhi, A. Hariharan, D. Goswami, and W. S. Warren, J. Chem. Phys. **101**, 6439 (1994).

[5] N. V. Vitanov, T. Halfmann, B. W. Shore, and K. Bergmann, Annu. Rev. Phys. Chem. **52**, 763 (2001).

[6] V. S. Malinovsky and J. L. Krause, Eur. Phys. J. D **14**, 147 (2001).

[7] R. P. Feynman, J. Frank, L. Vernon, and R. W. Hellwarth, J. Appl. Phys. **28**, 49 (1957).

[8] P. D. Featonby, G. S. Summy, J. L. Martin, H. Wu, K. P. Zetie, C. J. Foot, and K. Burnett, Phys. Rev. A **53**, 373 (1996).

[9] L. Mitschang and H. Rinneberg, J. Chem. Phys. **118**, 5496 (2003).

[10] J. Baum, R. Tycko, and A. Pines, Phys. Rev. A **32**, 3435 (1985).

[11] C. J. Hardy, W. A. Edelstein, and D. Vatis, J. Magn. Reson. (1969-1992) **66**, 470 (1986).

[12] B. W. Shore, *Simple Atoms and Fields*, Vol. 1 of *The Theory of Coherent Atomic Excitation* (John Wiley & Sons, 1989), ISBN 0-471-61398-3.

[13] H. J. Metcalf and P. van der Straten, *Laser Cooling and Trapping*, in Graduate Texts in Contemporary Physics (Springer, New York, 1999), ISBN 0-387-98747-9.

[14] C. N. Cohen-Tannoudji, B. Diu, and F. Laloë, *Quantum Mechanics* (John Wiley & Sons, New York, 1977), Vol. 1, ISBN 0-471-16433-X.

[15] D. Rosenfeld and Y. Zur, J. Magn. Reson. **132**, 102 (1998).

[16] T. Lu, X. Miao, and H. Metcalf, Phys. Rev. A **71**, 061405(R) (2005).

[17] D. Goswami and W. S. Warren, Phys. Rev. A **50**, 5190 (1994).

[18] W. H. Press, S. A. Teukolsky, W. T. Vetterling, and B. P. Flannery, *Numerical Recipes in C*, 2nd ed., (Cambridge University Press, Cambridge, England, 1992), ISBN 0-521-43108-5.

[19] C. D. Wallace, T. P. Dinneen, A. Kumarakrishnan, P. L. Gould, and J. Javanainen, J. Opt. Soc. Am. B **11**, 703 (1994).

[20] I. Dotsenko, W. Alt, S. Kuhr, D. Schrader, M. Muller, Y. Miroshnychenko, V. Gomer, A. Rauschenbeutel, and D. Meschede, Appl. Phys. B: Lasers Opt. **78**, 711 (2004).

[21] G. P. Djotyan, J. S. Bakos, G. Demeter, P. N. Ignácz, M. A. Kedves, Z. Sörlei, J. Szigeti, and Z. L. Tóth, Phys. Rev. A **68**, 053409 (2003).

[22] C. J. Foot, *Atomic Physics*, in Oxford Master Series in Atomic, Optical and Laser Physics (Oxford University Press, New York, 2005), ISBN 0-19-850695-3.

[23] L. P. Yatsenko, B. W. Shore, T. Halfmann, K. Bergmann, and A. Vardi, Phys. Rev. A **60**, R4237 (1999).

[24] T. Rickes, L. P. Yatsenko, S. Steuerwald, T. Halfmann, B. W. Shore, N. V. Vitanov, and K. Bergmann, J. Chem. Phys. **113**, 534 (2000).

[25] L. P. Yatsenko, N. V. Vitanov, B. W. Shore, T. Rickes, and K. Bergmann, Opt. Commun. **204**, 413 (2002).

[26] N. V. Vitanov and B. W. Shore, Phys. Rev. A **73**, 053402 (2006).

[27] Y. Wu, Phys. Rev. A **54**, 1586 (1996).

[28] P. Marte, P. Zoller, and J. L. Hall, Phys. Rev. A **44**, R4118 (1991).

[29] N. V. Vitanov, K. A. Suominen, and B. W. Shore, J. Phys. B **32**, 4535 (1999).

[30] We operate in the frequency modulation (FM) frame [10], which rotates at the instantaneous frequency of the pulse [15], and in which the direction of a field vector in the *xy* plane is fixed.